totic ($R \to 0$, $R \to \infty$) values is excellent. However, for $R = 0.5$ it was found necessary to improve the accuracy of the numerical calculations, since the other theories give values for the *ionization* energy not too different from the calculated one. The numerical integrations were, therefore, carried out using 120 and 250 points. The values obtained for $\Delta E/a$ were -1.084102 and -1.084097, respectively. Additionally, for $R = 1.0$ the integrations were done with 60 and 120 points. The values obtained were $-1.665\ 13$ and $-1.665\ 81$, respectively.

[12] It follows from this and the low-R behavior that the power series for $\Delta E/\alpha$ must have a finite radius of a convergence.

PHYSICAL REVIEW B VOLUME 5, NUMBER 8 15 APRIL 1972

Stress-Modulated Magnetoreflectivity of Gallium Antimonide and Gallium Arsenide†

M. Reine,*‡ R. L. Aggarwal, and B. Lax‡
Francis Bitter National Magnet Laboratory,§ Massachusetts Institute of Technology, Cambridge, Massachusetts 02139
(Received 24 November 1971)

We have employed the differential technique for stress modulation in an extensive study of low-temperature (30 K), interband magnetoreflectivity at the fundamental edge of GaSb and of GaAs. The data for GaSb were compared to the coupled-band theory of Pidgeon and Brown by means of an iterative "parameter-optimization" computer program. The following self-consistent set of band parameters was determined: $(m_c/m) = 0.042 \pm 0.001$; $(m_{1h}/m) = 0.042 \pm 0.002$; $(m_{hh}/m)_{100} = 0.29 \pm 0.09$; $(m_{hh}/m)_{110} = 0.36 \pm 0.13$; $(m_{hh}/m)_{111} = 0.40 \pm 0.16$; $\gamma_1^L = 13.3 \pm 0.4$; $\gamma_3^L = 5.7 \pm 0.2$; $\gamma_3^L - \gamma_2^L = 1.3 \pm 0.2$; $\kappa^L = 3.5 \pm 0.6$; $g_c = -7.8 \pm 0.8$; $E_p = (25 \pm 2)$ eV; and $F = -(1.5 \pm 0.5)\hbar^2/m$. Here m is the free-electron mass, m_c is the conduction-band effective mass, m_{1h} and m_{hh} are the light-hole and heavy-hole valence-band effective masses, γ_1^L, γ_2^L, γ_3^L, and κ^L are the Luttinger valence-band parameters, g_c is the conduction-band effective g factor, E_p is the interaction energy introduced by Kane, and F represents the interaction of the conduction band with higher-lying bands.

I. INTRODUCTION

We have employed the differential technique of stress modulation[1,2] in an extensive study of interband magnetoreflectivity at the fundamental edge of gallium antimonide and of gallium arsenide. The greatly enhanced sensitivity afforded by this technique has enabled us to obtain magnetooptical spectra of considerably greater detail and resolution than have previously been reported.[3–5] For example, for GaSb at 30 K transitions involving Landau levels as high as the 18th conduction-band level were observed over the spectral region from 0.8 to 1.25 eV.

The spectra for GaSb were quantitatively compared to the coupled-band theory of Pidgeon and Brown[6] by means of an iterative computer program based on a generalized least-squares method. The best fit of this theory to the experimental data yielded a self consistent set of band parameters for the conduction band, the light-hole and the heavy-hole valence bands, and the spin-orbit splitoff valence band.

This paper is organized as follows. The experimental details are contained in Sec. II. The theoretical results necessary for the analysis of the experimental spectra are summarized in Sec. III. The experimental results and their analysis for GaSb are presented in Sec. IV. The zero-field spectra for GaSb are discussed in Sec. IV A and the magnetooptical spectra are discussed in Sec. IV B. A preliminary analysis of the main features of the data based on the parabolic band theory of Roth *et al.*[7] is given in Sec. IV C. The detailed analysis of the data in terms of the coupled-band theory is described in Sec. IV D, and the set of band parameters thus obtained is compared with previous results in Sec. IV E. Finally, the experimental data for GaAs are presented and discussed in Sec. V.

II. EXPERIMENTAL DETAILS

The stress-modulation technique used in this work is essentially the same as that developed by Engeler *et al.*[1] and adapted for low-temperature experiments by Aggarwal.[2] This technique and the associated apparatus have previously been described.[2,8] Briefly, this consists of a thin sample bonded to a piezoelectric transducer with vacuum grease. The transducer is driven by an ac voltage at an audio frequency and the resulting modulation in the reflectivity is detected by a phase-sensitive technique.

Data were taken in both the Faraday and the Voigt configurations. For the Voigt configuration, linearly polarized light was obtained by means of Polaroid-type HN32 or HR sheet polarizers. For the Faraday configuration, circularly polarized light was obtained

by means of a glass Fresnel rhomb, together with the appropriate linear polarizer.

The gallium antimonide used in these experiments was obtained in single-crystal form (ingot No. L11) from Bell and Howell. The specifications furnished with the material stated that it was not intentionally doped and that it was p type with a carrier concentration of 1.3×10^{17} cm^{-3}, a resistivity of 0.0454 Ω cm, and a mobility of 1010 cm^2/V sec at 300 K. Reid *et al.*[9] have measured the temperature dependence of the Hall coefficient and mobility for p-type GaSb of comparable purity. From their data, we estimate that our samples had a hole concentration of 2×10^{16} cm^{-3} and a mobility of 3700 cm^2/V sec at 77 K. The ingot was oriented by x-ray diffraction and several samples in the form of thin rectangular parallelepipeds of approximate dimensions $15\times3\times1.5$ mm were cut. Samples which were to be used in the Faraday configuration were cut such that their large faces were either a {100}, {110}, or {111} plane. The long edges were along either a ⟨100⟩ or a ⟨110⟩ direction so that they could also be used for the Voigt configuration. The samples were lapped on both faces, mechanically polished, and then etched in a 10:1 solution of bromine and methanol for approximately 45 sec. The final thickness after etching was about 0.5 mm.

The gallium-arsenide sample was obtained from Lincoln Laboratory. It consisted of an epitaxial layer deposited on a GaAs substrate. The epitaxial layer was n type with an electron mobility of about 1×10^5 cm^2/V sec at 80 K. The sample surface was a {211} plane and had dimensions of 5×10 mm.

III. THEORETICAL BACKGROUND

GaSb and GaAs crystallize in the zinc-blende structure. The direct optical transitions which comprise the fundamental absorption edge of these materials occur at the zone center between a fourfold degenerate set of valence bands (the so-called light-hole and heavy-hole bands, both of which are twofold degenerate) and a twofold degenerate conduction band. While the effects of a magnetic field on the conduction band (at least in the parabolic band approximation) are relatively straightforward, the effects on the light-hole and heavy-hole valence bands are complicated by the degeneracy of these bands at the zone center. Luttinger[10] treated the problem of these four bands in a magnetic field by means of the effective-mass approximation for parabolic bands. His results were applied by Roth *et al.*[7] and by Burstein *et al.*[11] to the problem of interband magnetooptical transitions.

The application of a magnetic field removes the fourfold degeneracy of the valence bands at $k=0$ with the result that there are four series of Landau levels, one for each of the original unperturbed bands. These have been designated by Roth *et al.*[7] as the a^+, the a^-, the b^+, and the b^- series. The individual Landau levels within each series are designated by a quantum number n.

The energy of each individual level is a linear function of the applied magnetic field strength (a consequence of the parabolic-band approximation) and depends on the quantum number n and on the parameters γ_1^L, γ_2^L, γ_3^L, and κ^L as well as on the orientation of the magnetic field relative to the crystal axes. The parameters γ_1^L, γ_2^L, and γ_3^L, defined by Luttinger[10] represent sums of matrix elements and are related to the parameters A, B, and C of Dresselhaus *et al.*[12] as follows:

$$\gamma_1^L=A,\quad \gamma_2^L=\tfrac{1}{2}B,\quad \gamma_3^L=\tfrac{1}{2}(\tfrac{1}{3}C^2+B^2)^{1/2}. \tag{1}$$

The parameter κ^L is exclusive to the magnetic field problem and plays the role of an effective g factor. The following approximate expression[6] relates κ^L to the three γ^L's:

$$\kappa^L=\gamma_3^L+\tfrac{2}{3}\gamma_2^L-\tfrac{1}{3}\gamma_1^L-\tfrac{2}{3}. \tag{2}$$

The band-edge effective masses $m_{\rm lh}$ and $m_{\rm hh}$ for the light-hole and heavy-hole bands can be expressed in terms of these parameters as follows:

$$\left.\begin{matrix} m/m_{\rm lh} \\ m/m_{\rm hh} \end{matrix}\right\} =\gamma_1^L\pm[(\gamma'^L)^2+3(\gamma''^L)^2]^{1/2}, \tag{3}$$

where

$$\gamma'^L=\gamma_3^L-(\gamma_3^L-\gamma_2^L)f(\theta), \tag{4}$$

$$\gamma''^L=\gamma_3^L-\tfrac{1}{3}(\gamma_3^L-\gamma_2^L)[1+f(\theta)]. \tag{5}$$

The function $f(\theta)$ is given by

$$f(\theta)=\tfrac{1}{4}(3\cos^2\theta-1)^2, \tag{6}$$

where θ is the angle between the magnetic field and the [001] direction.

The selection rules and relative intensities for optical transitions from the magnetic levels of the valence bands to those of the conduction band were calculated by both Roth *et al.*[7] and Burstein *et al.*[11] These levels and representative allowed transitions are shown in Fig. 1. The conduction-band series for spin up is labeled a^c and that for spin down is labeled b^c. The b^c levels are slightly higher in energy due to the negative value of the conduction-band effective g factor. The levels of Fig. 1 are numbered according to the notation adopted by Pidgeon and Brown.[6] The levels of the a^+ and b^+ series begin with $n=-1$, while those of the a^- and the b^- series begin with $n=1$. For the Faraday configuration the following transitions are allowed:

$$a^\pm(n')\rightarrow a^c(n),\quad b^\pm(n')\rightarrow b^c(n). \tag{7}$$

The selection rules for these transitions are

$$\Delta n=n-n'=\begin{cases}+1 & \text{left circularly polarized (LCP)}\\ -1 & \text{right circularly polarized (RCP).}\end{cases} \tag{8}$$

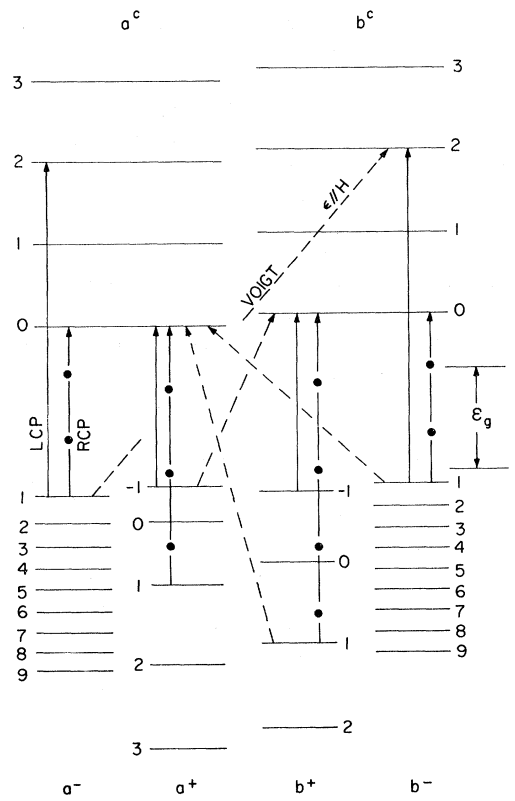

FIG. 1. Landau-level diagram for the conduction band and the light-hole and heavy-hole valence bands. The value of the Landau quantum number for each level is shown. The lowest-energy interband transitions allowed for the Faraday configuration (RCP and LCP) and for the Voigt configuration are indicated by the arrows.

For the Voigt configuration, the allowed transitions and selection rules are

$$a^{\pm}(n') \rightarrow b^{c}(n), \quad \Delta n = 1$$
$$b^{\pm}(n') \rightarrow a^{c}(n), \quad \Delta n = -1. \tag{9}$$

It should be pointed out that the above selection rule of $\Delta n = \pm 1$ corresponds to the selection $\Delta n = 0, -2$ in the notation of Roth *et al.*[7] The intensities of these transitions depend in general on the parameters γ_1^L, γ_2^L, γ_3^L, and κ^L and on the Landau quantum number of the valence-band level. Expressions for the intensities can readily be obtained from Eqs. (26) and (31) of Ref. 7. Qualitatively, transitions from both heavy-hole series should be strong in both RCP and LCP; transitions from the a^+ light-hole series occur mainly for RCP while those from the b^+ series occur mainly for LCP.

Because the calculations outlined above assumed parabolic bands, they predicted magnetooptical transition energies which were linear functions of the magnetic field strength. However, even the early magnetooptical experiments showed nonlinear dependence of transition energies on field strength. This meant that band nonparabolicity was important and had to be taken into account. Roth *et al.*[7] showed how nonparabolic terms could be treated as a perturbation on the parabolic problem. In a much more complete theory, however, Pidgeon and Brown[6] treated the conduction band, the light-hole and the heavy-hole valence bands, and the splitoff valence band, each doubly degenerate due to spin, as being all "nearly degenerate." In their formalism, the energies of the magnetic levels associated with each of the eight bands were solutions to a pair of 4×4 eigenvalue matrixes.

In addition to the Luttinger parameters γ_1^L, γ'^L, γ''^L, and κ^L, the Pidgeon-Brown formalism contains the following band-edge parameters: $\mathcal{E}_g$, the direct energy gap; Δ, the spin-orbit splitting; E_p, the conduction-band interaction energy defined by Kane[13]; and $F \equiv f(\hbar^2/m)$, a matrix element[13] representing the interaction of the conduction band with higher-lying bands. The effective mass m_c and the effective g factor g_c at the bottom of the conduction band can be expressed[14] in terms of these parameters as follows;

$$\frac{m}{m_c} = 1 + \frac{E_p}{3}\left(\frac{2}{\mathcal{E}_g} + \frac{1}{\mathcal{E}_g + \Delta}\right) + 2f,$$
$$g_c = 2\left[1 - \frac{E_p}{3}\left(\frac{1}{\mathcal{E}_g} - \frac{1}{\mathcal{E}_g + \Delta}\right)\right]. \tag{10}$$

Similarly, the corresponding band-edge effective mass m_{so} and effective g factor g_{so} at the top of the splitoff band are given by

$$\frac{m}{m_{so}} = \gamma_1^L - \frac{E_p}{3}\left(\frac{1}{\mathcal{E}_g} - \frac{1}{\mathcal{E}_g + \Delta}\right),$$
$$g_{so} = -2\left[2\kappa^L + 1 - \frac{E_p}{3}\left(\frac{1}{\mathcal{E}_g} - \frac{1}{\mathcal{E}_g + \Delta}\right)\right]. \tag{11}$$

It is interesting that the sum of g_c and g_{so}, as given by Eqs. (10) and (11), is just equal to $-4\kappa^L$.

IV. GALLIUM ANTIMONIDE

A. Zero-Field Spectra

The stress-modulated reflectivity spectrum for the fundamental edge of GaSb is shown in Fig. 2 for sample temperatures of 77 and 30 K. The stress-modulated spectrum consists of the quantity $(1/R) \times (\Delta R/\Delta S)$ plotted as a function of photon energy. Here R is the reflectivity at near-normal incidence and ΔR is the rms change in R due to the application of a uniform two-dimensional strain of rms magnitude ΔS in the plane of the sample. As shown in Fig. 2, the spectra at 30 K were much sharper than those at 77 K; consequently all data were taken at the lower temperature.

The structure in the 30-K spectrum of Fig. 2 can be correlated with corresponding structure in the fundamental-edge absorption spectrum. Johnson

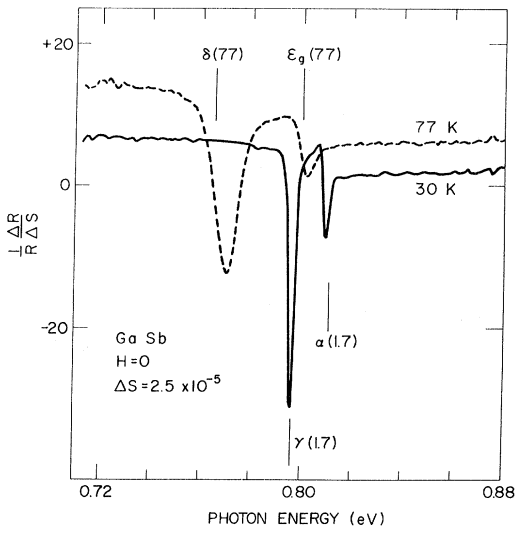

FIG. 2. Stress-modulated reflectivity spectrum at the fundamental edge of GaSb for $H=0$ and for temperatures of 30 and 77 K.

et al.[15,16] measured the absorption coefficient of undoped p-type GaSb under high resolution and at low temperature (1.7 and 4.2 K) in this spectral region. They were able to resolve three absorption peaks which they labeled α, β, and γ and which at 1.7 K occurred at energies of 0.8109, 0.8058, and 0.7967 eV, respectively. Since Zwerdling *et al.*[3] had already measured the energy gap $\mathcal{E}_g$ to be (0.813 ± 0.001) eV at 4 K, Johnson *et al.*[15,16] interpreted the α peak as optical absorption involving the creation of free excitons, and the lower energy β and γ peaks as absorption involving the creation of excitons bound to impurities (impurity-exciton complexes). More recently, Guillaume and Lavallard[17] have made a detailed study of radiative recombination from these exciton-impurity complexes in GaSb. They have concluded that both the β as well as the γ complexes consist of excitons bound to neutral acceptors.

The vertical lines in Fig. 2 show the energies of the α and the γ absorption peaks[15,16] at 1.7 K. Since these energies agree well with those of the sharp minima in the spectrum, we identify these minima as being associated with the free-exciton transition and the γ bound-excitation transition. However, there is no analogous structure in the spectrum which might correspond to the β bound-exciton transition. It should be pointed out that Pollak and Aggarwal[18] have measured the wavelength-modulated reflectivity spectrum at the fundamental edge of GaSb at 1.7 K. Their samples were comparable in purity to those used in this work. There was no evidence in their spectra for any structure corresponding to the β bound-exciton transition. This implies that the particular acceptor species responsible for the β complex is perhaps absent in higher-purity material.

In addition to the three absorption peaks, Johnson *et al.*[15,16] also observed a weak-absorption tail beginning at ~0.765 eV which they labeled δ. This type of absorption is characteristic of transitions in which the initial or final state is an impurity level. The photoconductivity experiments of Habegger and Fan[19] as well as radiative recombination studies[15,17] in undoped p-type GaSb indicate that there is in fact an impurity level at an energy of 0.034–0.035 eV above the valence-band edge at both 77 and 4.2 K. Structure corresponding to this impurity transition is seen clearly in the 77-K spectrum of Fig. 2. Although not shown in the 30-K spectrum of Fig. 2, we have occasionally observed this structure at 30 K. The value for $\mathcal{E}_g$ at 77 K, as measured by Becker *et al.*[20] from the position of the optical-absorption edge, is 0.80 eV and is indicated along with the position of the δ-impurity transition in Fig. 2. The structure in the 77-K spectrum near $\mathcal{E}_g$ is similar to that reported by Gavini and Cardona[21] and can be associated with the thermally broadened α exciton transition.

B. Magnetooptical Spectra

The application of a large magnetic field has a dramatic effect on the modulated-reflectivity spectrum of GaSb in the region of photon energies just above the energy gap. This is illustrated in Fig. 3 for a sample at ~30 K in a magnetic field of 88.5 kG. The spectra were taken for the Faraday configuration with the magnetic field normal to the reflecting sample surface and parallel to the ⟨100⟩ sample axis, and with the incident radiation either RCP or LCP. Figure 4 shows the corresponding spectra for a GaSb sample having a {111} reflecting surface with the magnetic field parallel to the ⟨111⟩ direction. Spectra were also taken for a {110} sample in the Faraday configuration.

The dominant features of the modulated magnetoreflectivity spectra of Figs. 3 and 4 are the negative peaks. With the exception of the structure labeled γ and δ, these peaks correspond to optical transitions from the Landau levels of the light-hole and heavy-hole valence bands to those of the conduction band.[22] The peaks are quite sharp (~2–3 meV wide) and intense at energies just above the energy gap ($\mathcal{E}_g \approx 0.81$ eV) and become weaker and broader with increasing energy. This is the usual behavior for the interband magnetooptical spectra and reflects the decrease in the lifetime of the optically excited electron with increasing Landau quantum number. The data of Figs. 3 and 4 are about 20–40 times more intense than the corresponding data[2] for Ge and represent the most sophisticated stress-modulated magnetoreflectivity data yet obtained. In the ⟨100⟩ RCP spectrum, for example, evidence of

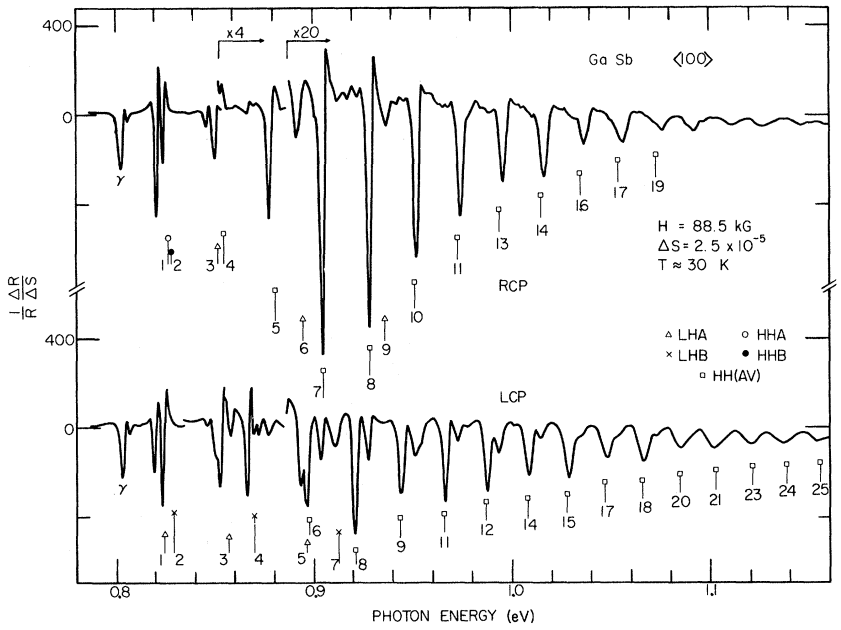

FIG. 3. Stress-modulated reflectivity spectra for GaSb in the Faraday configuration with the magnetic field along the ⟨100⟩ direction.

transitions persisted as far as 1.25 eV, or about 450 meV above the energy gap, and transitions to levels as high as the 18th conduction-band level could clearly be seen.

The structure labeled γ and δ in Figs. 3 and 4 correspond to the γ bound-exciton transition and the δ-impurity transition which were discussed in Sec. IV A. This structure is shown in more detail in Fig. 5 for $H = 0$ as well as for $H = 88.5$ kG in the ⟨111⟩ Faraday configuration. The γ peak is shifted to higher energy by the magnetic field and becomes less intense. The δ peak also shifts to higher energy by the same amount but becomes more intense and exhibits a small shoulder on the high-energy side. On the other hand, the free-exciton transition labeled α gives rise to the large number of Landau-level transitions shown in Fig. 3 and 4. For comparison, the lowest two of these transitions are also shown in Fig. 5 and are labeled 1 and 2.

A quantitative interpretation of the spectra of Figs. 3–5 requires the assignment of the energy of some particular feature of each negative peak,

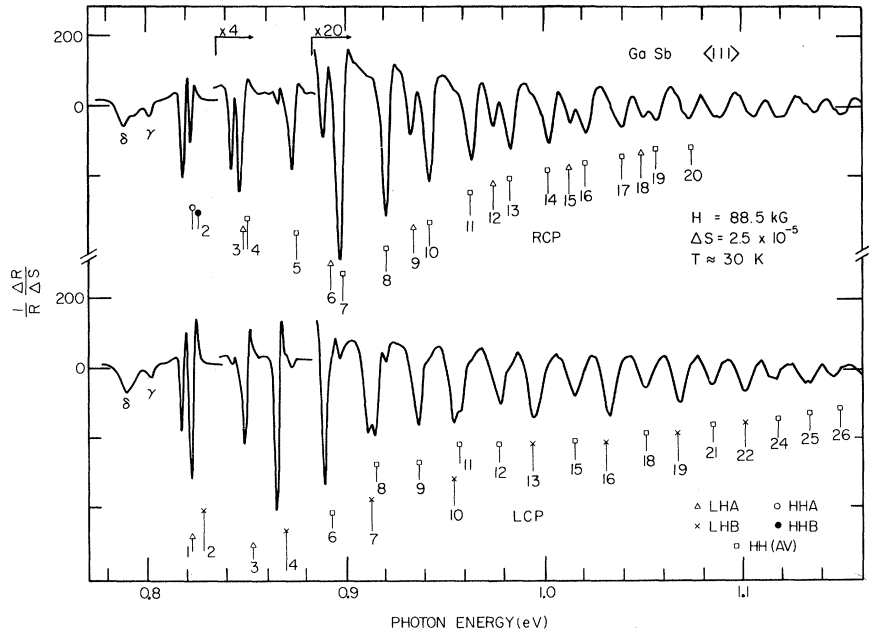

FIG. 4. Stress-modulated reflectivity spectra for GaSb in the Faraday configuration with the magnetic field along the ⟨111⟩ direction.

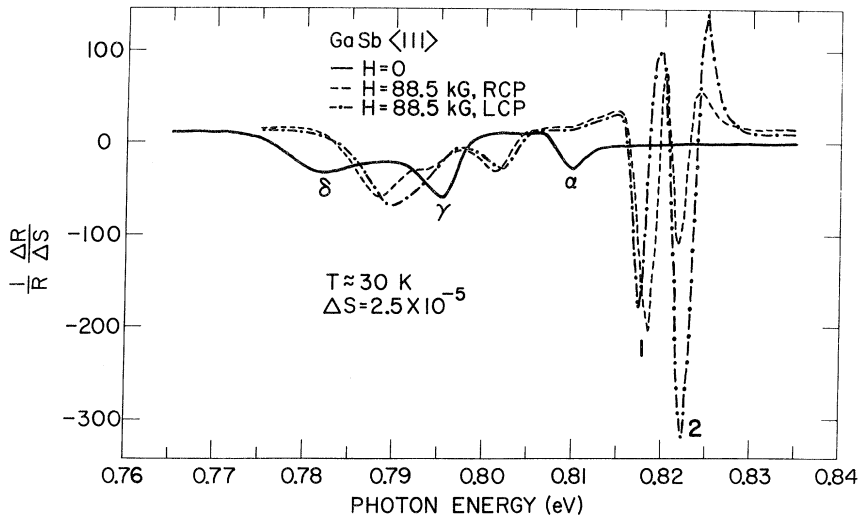

FIG. 5. Stress-modulated reflectivity spectra for GaSb for $H=0$ and for $H=88.5$ kG in the ⟨111⟩ Faraday configuration.

such as the minimum or an inflection point or, for the lowest few transitions, the maximum, as the energy of the transition with which the negative peak is associated. In the present analysis the energies of the minima of the negative peaks were chosen as the transition energies for several reasons. First of all, an inspection of Figs. 3–5 shows that the minimum is the best-defined feature of the structure. Second, Mavroides[23] has plotted the minimum, the maximum, and the inflection points for a transition in the stress-modulated magnetoreflectivity spectrum of Ge as a function of magnetic field and has shown that the slope of the minimum points most closely agrees with the theoretical slope calculated on the basis of the relatively well-known Ge band parameters. And finally, this criterion has successfully been used in the interpretation of the stress-modulated magnetoreflectivity data for Ge.[2]

This criterion has been used to obtain the behavior of the γ and δ transitions as a function of magnetic field. This is shown in Fig. 6 along with the behavior of the Landau-level transitions labeled 1 and 2. The behavior of these two transitions is consistent with that observed by Johnson *et al.*[15,16] at 21.6 kG and by Guillaume and Lavallard[17] at 50 kG. These two transitions will be discussed later in more detail. However, Fig. 6 shows that the γ transition has very nearly the same energy in both the RCP and LCP spectra, while Johnson *et al.*[15,16] observed a splitting of this transition of about 1.2 meV at 21.6 kG. This would imply a splitting of about 4.9 meV at our highest field of 88.5 kG, which is definitely not observed.

The data of Fig. 5 represent the first observation of the Zeeman effect of the δ-impurity transitions. Figure 6 shows an energy difference of about 1 meV between the RCP and LCP positions at 88.5 kG. In addition, the energy of the shoulder is about 4.3 meV above the stronger minimum at 88.5 kG. This splitting most probably corresponds to the spin-splitting of the lowest conduction-band Landau lev-

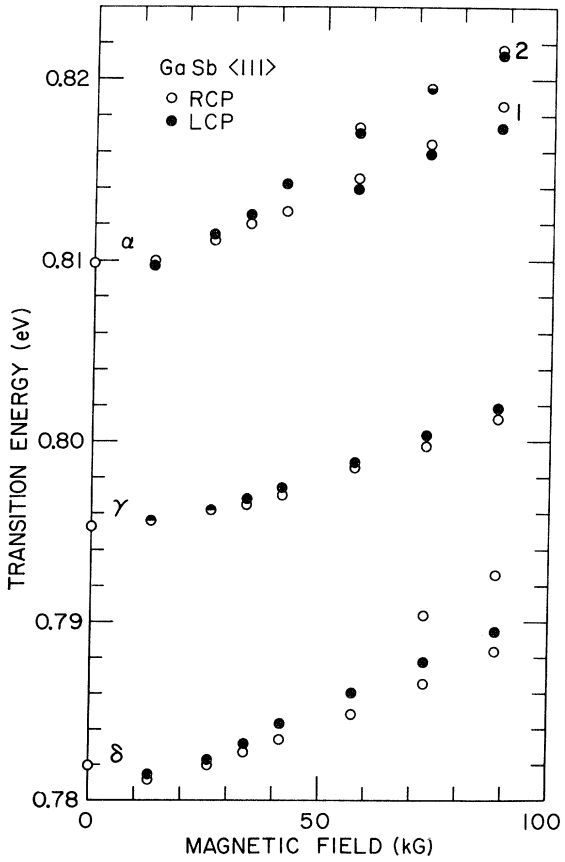

FIG. 6. Energies of the transition shown in Fig. 5 plotted as a function of magnetic field strength.

TABLE I. Experimentally observed transitions for GaSb in the Faraday configuration.

Label	Identification RCP	LCP
1	$a^-(1)a^c(0)$	$a^+(-1)a^c(0)$
2	$b^-(1)b^c(0)$	$b^+(-1)b^c(0)$
3	$a^+(1)a^c(0)$	$a^+(0)a^c(1)$
4	$a^-(2)a^c(1)$, $b^-(2)b^c(1)$	$b^+(0)b^c(1)$
5	$a^-(3)a^c(2)$, $b^-(3)b^c(2)$	$a^+(1)a^c(2)$
6	$a^+(2)a^c(1)$	$a^-(2)a^c(3)$, $b^-(2)b^c(3)$
7	$a^-(4)a^c(3)$, $b^-(4)b^c(3)$	$b^+(1)b^c(2)$
8	$a^-(5)a^c(4)$, $b^-(5)b^c(4)$	$a^-(3)a^c(4)$, $b^-(3)b^c(4)$
9	$a^+(3)a^c(2)$	$a^-(4)a^c(5)$, $b^-(4)b^c(5)$
10	$a^-(6)a^c(5)$, $b^-(6)b^c(5)$	$b^+(2)b^c(3)$
11	$a^-(7)a^c(6)$, $b^-(7)b^c(6)$	$a^-(5)a^c(6)$, $b^-(5)b^c(6)$
12	$a^+(4)a^c(3)$	$a^-(6)a^c(7)$, $b^-(6)b^c(7)$
13	$a^-(8)a^c(7)$, $b^-(8)b^c(7)$	$b^+(3)b^c(4)$
14	$a^-(9)a^c(8)$, $b^-(9)b^c(8)$	$a^-(7)a^c(8)$, $b^-(7)b^c(8)$
15	$a^+(5)a^c(4)$	$a^-(8)a^c(9)$, $b^-(8)b^c(9)$
16	$a^-(10)a^c(9)$, $b^-(10)b^c(9)$	$b^+(4)b^c(5)$
17	$a^-(11)a^c(10)$, $b^-(11)b^c(10)$	$a^-(9)a^c(10)$, $b^-(9)b^c(10)$
18	$a^+(6)a^c(5)$	$a^-(10)a^c(11)$, $b^-(10)b^c(11)$
19	$a^-(12)a^c(11)$, $b^-(12)b^c(11)$	$b^+(5)b^c(6)$
20	$a^-(13)a^c(12)$, $b^-(13)b^c(12)$	$a^-(11)a^c(12)$, $b^-(11)b^c(12)$
21		$a^-(12)a^c(13)$, $b^-(12)b^c(13)$
22		$b^+(6)b^c(7)$
23		$a^-(13)a^c(14)$, $b^-(13)b^c(14)$
24		$a^-(14)a^c(15)$, $b^-(14)b^c(15)$
25		$a^-(15)a^c(16)$, $b^-(15)b^c(16)$
26		$a^-(16)a^c(17)$, $b^-(16)b^c(17)$

el, in which case the data yield an estimate of 8.4 for the magnitude of the conduction-band effective g factor. This is in good agreement with the value of 7.8 ± 0.8 determined in Sec. IV D of this paper.

As mentioned earlier, the higher-energy negative peaks are associated with optical transitions between pairs of Landau levels in the valence and conduction bands. These transitions were identified by means of the selection rules of Roth *et al.*[7] summarized in Eqs. (7)–(9). This identification is indicated in Figs. 3 and 4 by means of the vertical line, the symbol and the number lying below each prominent peak. The position of the line indicates the theoretically predicted energy of the transition with which the peak is associated; the details of how the theoretical positions are obtained will be discussed in Sections IV C and IV D. The length of the line indicates the theoretical relative intensity of the transition. The symbol denotes the nature of the valence-band Landau level as being a light-hole (LHA) or heavy-hole (HHA) level of the a set, or a light-hole (LHB) or a heavy hole (HHB) level of the b set. In almost all cases the heavy-hole transitions of the a set and the corresponding heavy-hole transitions of the b set were too close to each other in energy to be resolved in the spectra. The theoretically predicted energy of a heavy-hole transition in the a set and of its counterpart in the b set turned out to be within at most ~2 meV of each other. The averages of the two energies are shown in Figs. 3 and 4 and are denoted by the symbol HH(AV). The numbers near the bottom of each vertical line refer to Table I, which gives for each transition the specific identification of the valence- and conduction-band levels involved. For example, $a^+(n')a^c(n)$ denotes a transition from the n'th light-hole level in the a set to the nth conduction-band level in the a set. For unresolved heavy-hole transitions, both pairs of levels are given. The numbering of the levels is as shown in Fig. 1.

Not all of the transitions which are allowed by the selection rules of Roth *et al.*[7] and which have energies in the spectral region investigated were observed. For some of these transitions, such as the $b^+(n')b^c(n)$ in RCP, the intensities are very much smaller than those of other allowed transitions. In addition, in the ⟨100⟩ RCP spectrum the light-hole $a^+(n')a^c(n)$ transitions are obscured because of their coincidence with alternate heavy-hole transitions. These light-hole transitions emerge clearly in the ⟨111⟩ RCP spectrum, for which the heavy-hole mass is slightly different. Another difficulty arises because of incomplete polarization of the incident radiation. This is particularly noticeable for transitions 7 and 8 in RCP; because of their large intensities, they also appear in the LCP spectrum. A comparison of their intensities in RCP and LCP indicates that the Fresnel rhomb produced a beam which was about 85% polarized. This probably obscured several of the higher-energy $b^+(n')b^c(n)$ transitions in the ⟨100⟩ LCP spectrum.

The stress-modulated magnetoreflectivity spectrum for GaSb at 30 K in the Voigt configuration is shown in Fig. 7. In this case linearly polarized light was incident on a {100} sample surface with the polarization vector parallel to the magnetic field applied along a ⟨110⟩ direction. The structure in the spectrum is considerably weaker and broader than that of the Faraday spectra. Even so, the minima of the spectra correspond to certain theoretically predicted transitions which are listed in Table II. These are all consistent with the selection rules of Eqs. (9). Because the structure broadened rapidly with increasing photon energy, it was not possible to

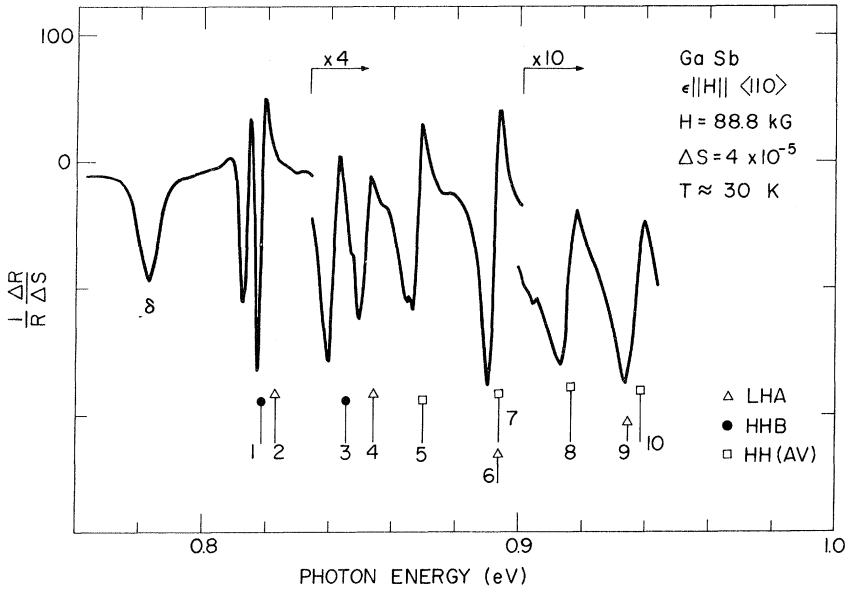

FIG. 7. Stress-modulated reflectivity spectrum for GaSb in the Voigt configuration with both the magnetic field and the polarization vector of the incident radiation parallel to the ⟨110⟩ direction.

carry this correspondence beyond the first ten transitions.

C. Preliminary Analysis

Because the data of Figs. 3, 4, and 7 extend to energies well above the conduction-band minimum, a proper analysis of these data can only be done within the coupled-band formalism of Pidgeon and Brown.[6] The results of such an analysis performed with the aid of a computer will be described in Sec. IV D. In this section we analyze certain simple features of the data in terms of the theory of Roth *et al.*[7]

Of particular interest are the transitions $a^+(0)a^c(1)$ and $b^+(0)b^c(1)$ which occur for LCP in the Faraday configuration and which are labeled 3 and 4 in Figs. 3 and 4. Their observed dependence on magnetic field is shown in Fig. 8 and is linear to within experimental error; presumably they are not so strongly influenced by exciton effects as are the lowest two transitions. The energies $\mathcal{E}(3)$ and $\mathcal{E}(4)$ of these transitions are given by

$$\mathcal{E}(3) = \mathcal{E}_g + \delta\mathcal{E}_g - \epsilon_1 + \tfrac{1}{2}s[(3m/m_c) + \tfrac{1}{2}g_c + 3\gamma_1^L - 3\gamma'^L - \kappa^L], \quad (12)$$

$$\mathcal{E}(4) = \mathcal{E}_g + \delta\mathcal{E}_g + \epsilon_1 + \tfrac{1}{2}s\,(m/m_c - \tfrac{1}{2}g_c + 3\gamma_1^L + 3\gamma'^L - 3\kappa^L), \quad (13)$$

TABLE II. Experimentally observed transitions for GaSb in the Voigt configuration.

Label	Identification
1	$b^-(1)a^c(0)$
2	$a^+(-1)b^c(0)$
3	$b^-(2)a^c(1)$
4	$a^+(0)b^c(1)$
5	$a^-(1)b^c(2)$, $b^-(3)a^c(2)$
6	$a^+(1)b^c(2)$
7	$a^-(2)b^c(3)$, $b^-(4)a^c(3)$
8	$a^-(3)b^c(4)$, $b^-(5)a^c(4)$
9	$a^+(2)b^c(3)$
10	$a^-(4)b^c(5)$, $b^-(6)a^c(5)$

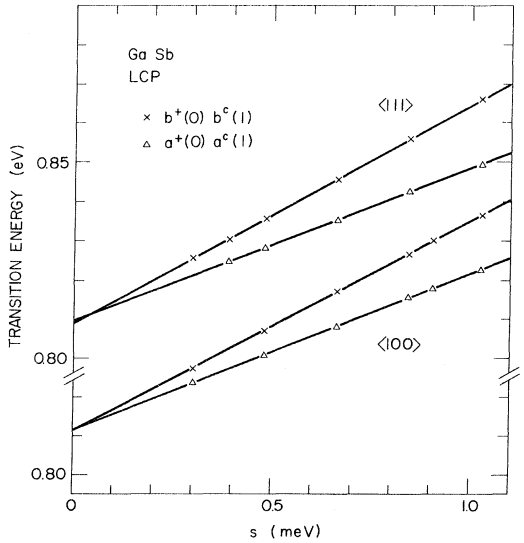

FIG. 8. Light-hole transitions $a^+(0)a^c(1)$ and $b^+(0)b^c(1)$ observed in the LCP spectra of GaSb plotted against the quantity $s = \hbar eH/m_c$.

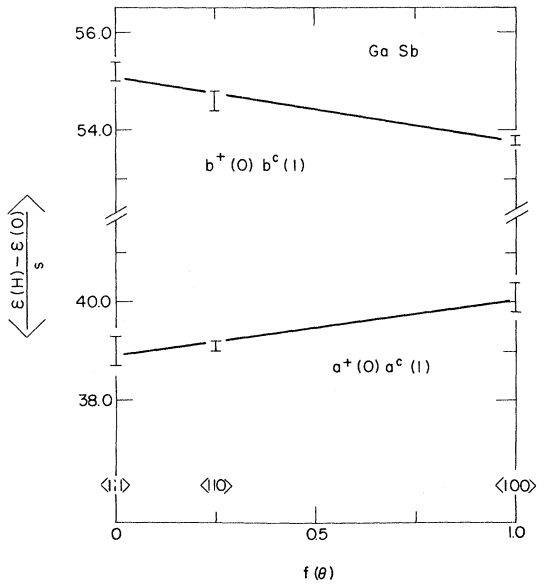

FIG. 9. Slopes of the energies of the light-hole transitions $a^+(0)a^c(1)$ and $b^+(0)b^c(1)$ as functions of magnetic field are shown plotted for the three main orientations against the function $f(\theta)$ defined in Eq. (6). The straight lines are least-squares fits to the points.

where $\mathcal{E}_g$ is the energy gap, $\delta\mathcal{E}_g$ and ϵ_1 are strain-induced energy shifts as defined in Ref. 2, $s=\hbar eH/m_c$, m_c is the conduction-band-edge effective mass, g_c is the conduction-band-edge effective g factor, and γ_1^L, γ'^L, and κ^L are the valence-band parameters introduced by Luttinger.[10]

The experimentally determined energies for these two transitions for both the ⟨100⟩ and the ⟨111⟩ data are shown plotted against the quantity s in Fig. 8. From Eqs. (12) and (13), the difference in the intercepts at $s=0$ of $\mathcal{E}(3)$ and $\mathcal{E}(4)$ is just $2\epsilon_1$, the strain splitting of the valence-band edge. The differences in the intercepts at $s=0$ in Fig. 8 are quite small and give $2\epsilon_1=0.3$ meV for the ⟨100⟩ data and $2\epsilon_1=0.7$ meV for the ⟨111⟩ data. These values indicate that the magnitude of the dc strain was comparable to that of the ac modulating strain. In view of this, the effects of the dc strain were neglected.

The slopes of the transition energies $\mathcal{E}(3)$ and $\mathcal{E}(4)$ as functions of s are expressed in Eqs. (12) and (13) in terms of certain combinations of the band parameters. The only parameter which depends on the orientation of the magnetic field relative to the crystal axes is γ'^L, which is defined in terms of γ_2^L and γ_3^L in Eq. (4). Consequently, if the slopes of the transition energies $\mathcal{E}(3)$ and $\mathcal{E}(4)$ for various orientations of the magnetic field are plotted against the function $f(\theta)$, the result should be straight lines with slopes $+\frac{3}{2}(\gamma_3^L-\gamma_2^L)$ for the $\mathcal{E}(3)$ points and $-\frac{3}{2}(\gamma_3^L-\gamma_2^L)$ for the $\mathcal{E}(4)$ points. Such a plot is shown in Fig. 9 for the magnetic field along the ⟨100⟩, ⟨111⟩, and ⟨110⟩ directions. The straight lines shown are least-squares fits to the points and their slopes give the following result:

$$\gamma_3^L-\gamma_2^L=0.8\pm0.1. \tag{14}$$

The transition $a^+(0)b^c(1)$ occurs in the Voigt configuration and involves the same light-hole valence-band level as does the transition $a^+(0)a^c(1)$ in the Faraday configuration for LCP. The conduction-band levels have the same quantum number but are of different spin, so that the difference between the slopes of the transition energies as functions of s should just be equal to the conduction-band effective g factor g_c. The experimentally determined slope for the $a^+(0)b^c(1)$ transition in the Voigt configuration is 39.1 ± 0.1. Since the magnetic field was along the ⟨100⟩ direction for the Voigt data, this should be compared with the slope for the $a^+(0)a^c(1)$ transition in the ⟨110⟩ Faraday data. This slope was 41.9 ± 0.4, so that a value of -5.6 ± 1.0 for g_c is deduced. It should be noted that the value for g_c and the above value for $(\gamma_3^L-\gamma_2^L)$ are not entirely reliable in view of the unknown extent to which the two transition energies are affected by excitons. These values will be discussed further in Sec. IV D and IV E.

Because of the relatively large heavy-hole mass, the nonlinear dependence of the heavy-hole transition energies on magnetic field is due mainly to the nonparabolicity of the conduction band. The spacing between adjacent heavy-hole levels is essentially constant for large quantum numbers and is given by $s(m/m_{hh})$, where m_{hh} is the heavy-hole valence-band effective mass. Nonparabolicity causes the spacing between adjacent conduction-band levels to become smaller for higher quantum numbers. Kane's theory[13] gives the following expression for the conduction-band energy $\mathcal{E}_c$:

$$\mathcal{E}_c=\mathcal{E}_g+\frac{\hbar^2k^2}{2m_c}-\left(\frac{\hbar^2k^2}{2m}\right)^2 p, \tag{15}$$

$$p=\left(\frac{m}{m_c}-1\right)^2\left(\frac{3+4Q+2Q^2}{3+5Q+2Q^2}\right)\frac{1}{\mathcal{E}_g}, \tag{16}$$

where $Q=\Delta/\mathcal{E}_g$. The conduction-band levels in a magnetic field are obtained by replacing $(\hbar^2k^2/2m)$ by $(n+\frac{1}{2})s$. The difference between the nth and the $(n-1)$th conduction-band levels is $s(m/m_c-2nsp)$, and hence the difference $\Delta\mathcal{E}(n)$ between the heavy-hole transitions $a^-(n')a^c(n)$ and $a^-(n'-1)a^c(n-1)$ or $b^-(n')b^c(n)$ and $b^-(n')b^c(n-1)$ is given by

$$\Delta\mathcal{E}(n)=s\left(\frac{m}{m_c}+\frac{m}{m_{hh}}-2nsp\right). \tag{17}$$

According to Eq. (17), if the quantity $\Delta\mathcal{E}(n)/s$ is plotted against n, a straight line should result with an intercept at $n=0$ equal to $(m/m_c+m/m_{hh})$. This was done for several heavy-hole transitions ob-

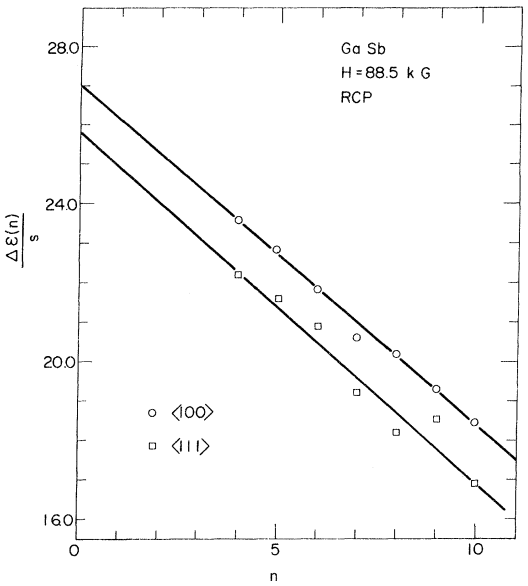

FIG. 10. Quantity $\Delta\mathcal{E}(n)$ is the energy difference between two adjacent heavy-hole transitions, n is the Landau quantum number of the conduction band of the higher of the two transitions, and $s = \hbar eH/m_c$. The plot illustrates the nonparabolicity of the conduction band; the quantity $\Delta\mathcal{E}(n)$ would be independent of n if the conduction band were purely parabolic.

served in the Faraday configuration for RCP and the results are shown in Fig. 10. The lowest few transitions were not used because of the irregular spacing of the lower heavy-hole levels and because of possible exciton effects, and the highest few transitions were not used because of their broader line shapes. The straight lines in Fig. 10 are least-squares fits to the points. Their intercepts at $n = 0$ are 27.0 for the ⟨100⟩ data and 25.8 for the ⟨111⟩ data, which provide the following values for the reduced effective mass μ for the conduction and heavy-hole bands:

$$\frac{\mu}{m} = \begin{cases} 0.037 \pm 0.001\,, & \langle 100\rangle \\ 0.039 \pm 0.001\,, & \langle 111\rangle\,. \end{cases} \qquad (18)$$

The difference in the values for the two orientations expresses the anisotropy of the heavy-hole band and shows that the effective mass in the {111} plane is larger than that in the {100} plane. This is consistent with the result of Eq. (14) that $\gamma_3^L > \gamma_2^L$. Zwerdling *et al.*[3] quoted $(\mu/m) = 0.042 \pm 0.002$ for a ⟨111⟩ orientation, which is significantly larger than the preliminary value in Eq. (18).

The values of Eq. (18) can be combined with Stradling's cyclotron-resonance values[24] for m_{hh} to obtain a preliminary value for m_c. He found $(m_{hh}/m) = 0.26 \pm 0.04$ and 0.36 ± 0.03 for the ⟨100⟩ and ⟨111⟩ orientations. For each of these values Eqs. (18) give $m_c = 0.043m$, which is ~10% lower than the value of 0.047 obtained from the reduced mass of Zwerdling *et al.*[3] The slopes of the straight lines of Fig. 10 are nearly equal and, according to Eq. 17, give $2sp = 0.88$. For $H = 88.5$ kG, the cyclotron energy s is 1.025 meV, so that $p = 0.43$ meV^{-1}. The value of p predicted by Eq. (16), for $\mathcal{E}_g = 0.81$ eV, $m_c = 0.043m$, and $Q = (\Delta/\mathcal{E}_g) \approx 1$, is 0.53 meV^{-1}, which is in fair agreement with the experimental result.

D. Detailed Analysis

A detailed analysis of the data, such as that shown in Figs. 3 and 4, in terms of the coupled-band theory of Pidgeon and Brown[6] is not straightforward. The procedure for obtaining the best agreement between theory and experiment is considerably complicated both by the nonanalytic form of the theoretical transition energies as well as by the large number of independent band parameters involved.

There are altogether 11 such parameters m_c, γ_1^L, γ_2^L, γ_3^L, κ^L, f, $\mathcal{E}_g$, Δ, the magnetic field strength, the Landau quantum number, and the orientation of the magnetic field with respect to the crystal axes. For a given transition the last three of these are known. In addition, the magnetic levels are sufficiently insensitive to $\mathcal{E}_g$ and Δ so that their previously determined values can be used. Finally, the Luttinger parameter κ^L can be expressed to a good approximation in terms of the γ^L's by means of Eq. (2). This leaves the five band parameters m_c, γ_1^L, γ_2^L, γ_3^L, and f to be determined by the experimental data. Of these five the most important are m_c, γ_1^L, and either γ_2^L, or γ_3^L, since the difference $(\gamma_3^L - \gamma_2^L)$ is small. The higher band parameter f is at best a very small correction.

For a given set of these five band parameters, two 4×4 eigenvalue matrixes must be solved by computer for each value of magnetic field and for each value of Landau quantum number. The theoretical transition energies must then be compared with the experimental points. In order to determine the best set of parameters, the process must be repeated for many combinations of parameter values and a combination giving the best over-all agreement to the experimental points must be chosen by some criterion. This trial and error method is inexact and time consuming.

In view of these difficulties, an iterative computerized approach based on a generalized method of least squares was adopted. A "parameter-optimization" program was written which accepted as input the experimental transition energies and initial values of the parameters m_c, γ_1^L, γ_3^L, $\mathcal{E}_g$, Δ, $(\gamma_3^L - \gamma_2^L)$, and f. The theoretical transition energies were calculated and compared to the experimental data. First-order correction terms were then generated for the three most important parameters

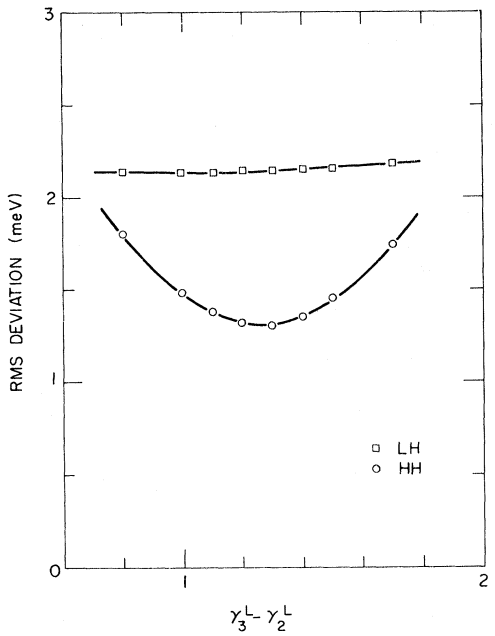

FIG. 11. The rms deviation between theory and experiment for light-hole (LH) and heavy-hole (HH) transitions, obtained from the iterative program for various values $(\gamma_3^L - \gamma_2^L)$. The minimum in the HH deviation determines the value 1.3 ± 0.2 for the difference $(\gamma_3^L - \gamma_2^L)$.

m_c, γ_1^L, and γ_3^L. This procedure was iterated until the parameters converged to their optimum values. In practice it was found that four to five iterations were sufficient for this purpose.[25]

In choosing the experimental transition energies to be used with the above program, the Voigt configuration data were excluded because of the broader spectral line shapes. Similarly, certain of the Faraday configuration data, such as the highest-energy transitions and some of the transition energies for lower magnetic fields, were not used because of their broader line shapes. In addition, the lowest four transitions were not used because of the strong influence of excitons.

The initial values for m_c, γ_1^L, and γ_3^L were taken from previous work. The value of $m_c = 0.047m$ was obtained from the magnetoabsorption study of Zwerdling *et al.*[3] and the values of $\gamma_1^L = 11.0$ and $\gamma_3^L = 4.4$ were taken from Stradling's cyclotron-resonance work.[24] Initially the value of $(\gamma_3^L - \gamma_2^L) = 0.8$ from Eq. (14) was used and f was set equal to zero. It was found later, however, that a better agreement between theory and experiment could be achieved by using slightly different values for these two fixed parameters. This is illustrated in Fig. 11 for the case of the anisotropy parameter $(\gamma_3^L - \gamma_2^L)$. The rms deviation for the light-hole transitions is essentially constant but that for the heavy-hole transitions shows a definite minimum. This illustrates the much greater anisotropy of the heavy-hole mass. From the minimum in Fig. 11 the following value was determined:

$$\gamma_3^L - \gamma_2^L = 1.3 \pm 0.2. \tag{19}$$

This value is higher than that of 0.8 ± 0.1 obtained previously on the basis of the low-quantum-number transitions $a^+(0)a^c(1)$ and $b^+(0)b^c(1)$. This difference is most probably due to the effect of excitons on these two transitions. In any event the value of Eq. (19), based on a large number of high-quantum-number transitions, is certainly more reliable.

Similarly, it was found that a better fit for the light-hole transitions could be attained by using a nonzero value for the parameter f. Figure 12 shows the results for several negative values of f. The rms deviation for the light-hole transitions shows a minimum near $f = -1.5$. From this minimum the following value was determined:

$$f = -1.5 \pm 0.5 . \tag{20}$$

This is close to the value $f = -1.1 \pm 0.2$ obtained for Ge.[2]

With $\mathcal{E}_g = 0.8102$ eV,[25] $\Delta = 0.749$ eV,[26] $f = -1.5$, and $(\gamma_3^L - \gamma_2^L) = 1.3$, and with κ^L approximated in terms of the γ^L's by Eq. (2), the program converged to the following values: $m_c = 0.0418m$, $\gamma_1^L = 13.3$, and $\gamma_3^L = 5.7$. For these values Eq. (2) yields $\kappa^L = 3.5$ and Eq. (10) yields $E_p = 25$ eV. The total rms derivation between theory and experiment was 1.4 meV,

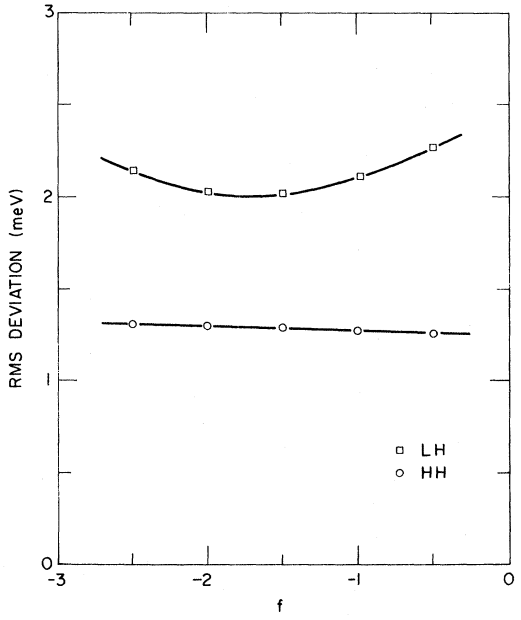

FIG. 12. The rms deviation between theory and experiment for light-hole (LH) and heavy-hole (HH) transitions, obtained from the iterative program for various values of the parameter f. The minimum in the LH deviation determines the value -1.5 ± 0.5 for f.

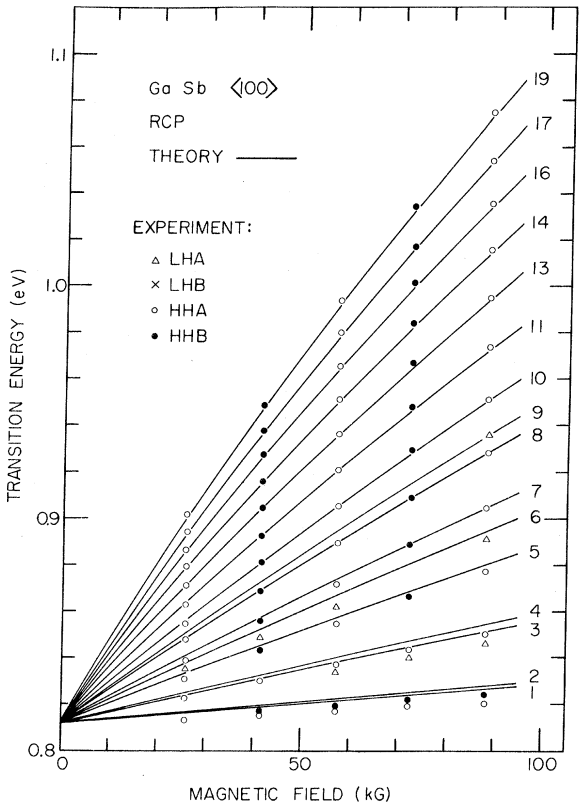

FIG. 13. Transition energies observed in the ⟨100⟩ GaSb spectrum for RCP radiation plotted against magnetic field.

while the rms deviation for the heavy-hole transitions was 1.3 meV and that for the light-hole transitions was 2.0 meV.

The theoretical transition energies calculated with the above set of band parameters are compared to the experimental data in Figs. 13–16. The numbers associated with each transition-energy curve are the same as those appearing in Figs. 3 and 4 and refer to the list of transition assignments given in Table I. For most of the heavy-hole transitions both the HHA and HHB symbols were used to indicate that the pair of heavy-hole transitions $a^-(n')a^c(n)$ and $b^-(n')b^c(n)$ was not resolved in the spectra. In calculating the theoretical transition energies the program automatically took the average energy of the heavy-hole transitions $a^-(n')a^c(n)$ and $b^-(n')b^c(n)$. The experimental points for the lowest four or five transitions in Figs. 13–16 lie several meV below the the theoretical curves and have slightly different slopes; this is presumably due to the larger influence of excitons on these transitions. Except for these transitions, the over-all agreement between theory and experiment is excellent. This is particularly so for the heavy-hole transitions.

The program converged to exactly the same values each time it was executed, irrespective of various combinations of initial values used. This indicated that the resulting minimum in the total rms deviation was both unique and well defined. In view of this we estimate an uncertainty of 3% in the values of m_c, γ_1^L, and γ_3^L. Thus the following values are determined:

$$m_c = (0.042 \pm 0.001)m, \qquad (21)$$
$$\gamma_1^L = 13.3 \pm 0.4, \quad \gamma_3^L = 5.7 \pm 0.2.$$

The light-hole effective mass calculated from Eqs. (3)–(5) for values of the γ^L's given by Eqs. (19) and (21) has the value $(0.042 \pm 0.002)m$. The calculated anisotropy in the light-hole mass is ~3%, which is small and is on the order of the estimated experimental error. On the other hand, the anisotropy of the heavy-hole mass is considerably larger. The values calculated from Eqs. (3)–(5) are

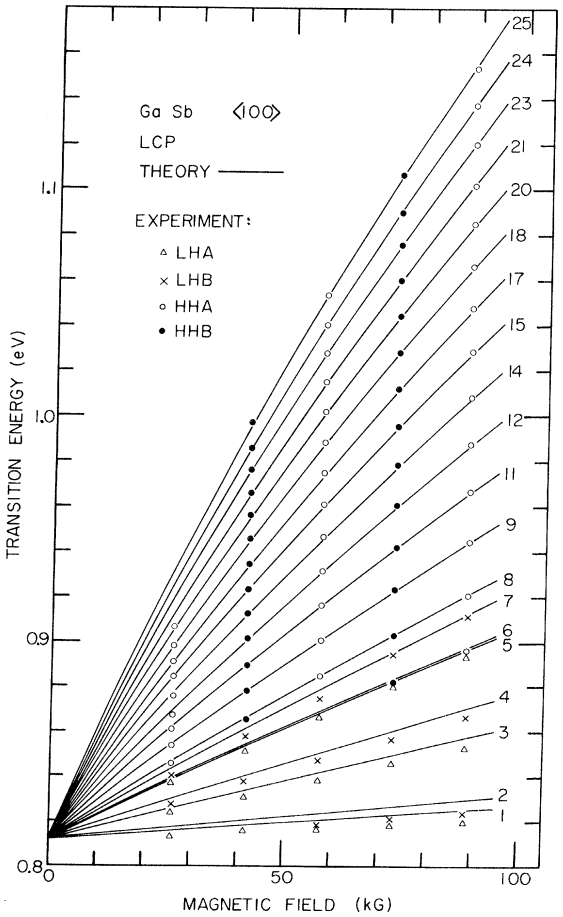

FIG. 14. Transitions observed in the ⟨100⟩ GaSb spectrum for LCP radiation plotted against magnetic field.

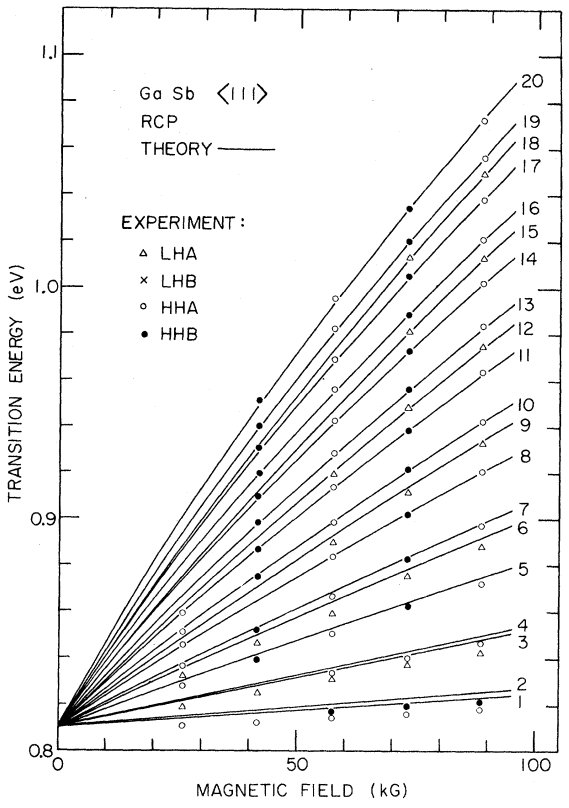

FIG. 15. Transitions observed in the ⟨111⟩ GaSb spectrum for RCP radiation plotted against magnetic field.

$$\left(\frac{m_{hh}}{m}\right) = \begin{cases} 0.29 \pm 0.09, & \langle 100 \rangle \\ 0.36 \pm 0.13, & \langle 110 \rangle \\ 0.40 \pm 0.16, & \langle 111 \rangle \ . \end{cases} \tag{22}$$

The resulting values for the reduced mass for the conduction and heavy-hole bands are $0.037m$ and $0.038m$ for the ⟨100⟩ and ⟨111⟩ directions. These agree with the values of Eq. (18) obtained by the analysis of the nonparabolicity of the heavy-hole transitions. The conduction-band effective g factor g_c, calculated from Eq. (10) with the above values, was -7.8 ± 0.8. This value of g_c differs from the value of -5.6 obtained from the analysis of the lowest few transitions given in Sec. IV C. The difference is no doubt due to the influence of excitons on these transitions. In particular, the above parameter values substituted into the left-hand sides of Eqs. (12) and (13) give the slopes as 43.9 and 47.8, as opposed to the experimentally observed values of 39.1 and 41.9. This decrease in slope is consistent with the increase in exciton binding energy with magnetic field as predicted by the calculations of Yafet *et al.*[27] and of Elliott and Loudon.[28]

E. Comparison with Previous Work

The self-consistent set of parameters for the conduction band and the light-hole and heavy-hole valence bands determined by the method of Sec. IV D are listed in Table III along with their estimated uncertainties. For comparison, Table III also shows the values of these parameters determined from both magnetoabsorption and cyclotron resonance, and from other experiments as well as from theory.

There have been two interband magnetoabsorption studies of thin (~4–8-μ) GaSb samples at low temperature. The first of these was done by Zwerdling *et al.*[3] They observed about nine transitions at their highest field of 40 kG and obtained a value of $(0.042 \pm 0.002)m$ for the reduced mass for the conduction and heavy-hole bands for a ⟨111⟩ orientation. Using a value for the heavy-hole mass between $0.38m$ and $0.56m$, they deduced the conduction-band mass value of $(0.047 \pm 0.003)m$ which appears in Table III. Later, Adachi[29] analyzed

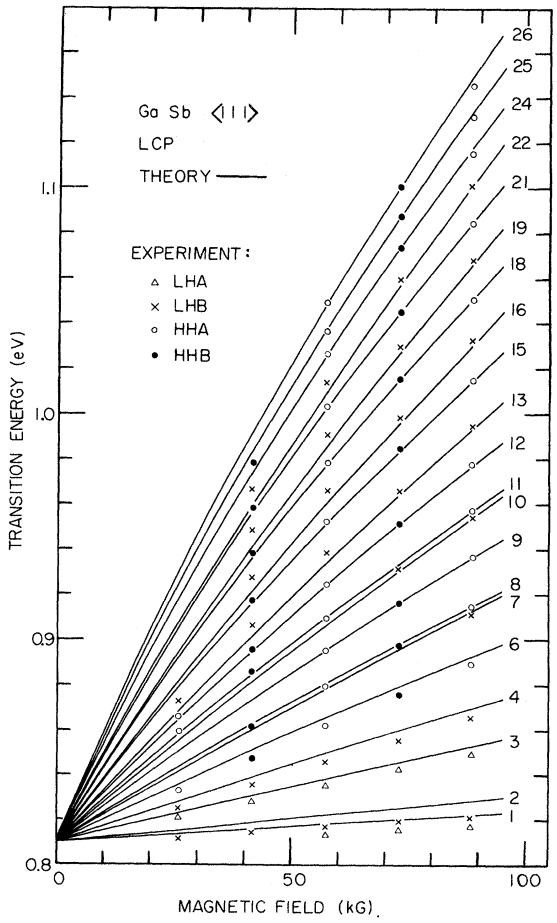

FIG. 16. Transitions observed in the ⟨111⟩ GaSb spectrum for LCP radiation plotted against magnetic field.

their data on the basis of the Pidgeon-Brown theory and obtained the values for m_c, m_{lh}, γ_1^L, γ_3^L, κ^L, and g_c listed in Table III. Halpern[30] extended Zwerdling's experiment up to fields of 100 kG. He was unable to observe very many more transitions but the data at higher magnetic fields definitely showed the effects of band nonparabolicity. Using a cyclotron-resonance value for the heavy-hole mass, Lax and Mavroides[31] estimated $m_c = 0.041m$ from this unpublished data.

Recent electron-cyclotron-resonance measurements in p-type GaSb at 1.7 K by Hill and Schwerdtfeger[32] have yielded the value of $(0.042 \pm 0.002)m$ for the conduction-band effective mass. This value is in excellent agreement with the value obtained from the present experiments. It is possible that Bordure's value[33] for m_c of $(0.048 \pm 0.002)m$ and Piller's value[34] of $(0.049 \pm 0.004)m$, both determined from free-carrier Faraday rotation experiments on n-type samples, are too large because of conduction-band nonparabolicity.

Stradling[24] has done cyclotron-resonance experiments on p-type GaSb and his values for m_{lh} and m_{hh} are given in Table III. He also quotes values for the parameters A, B, and C; the values of γ_1^L, γ_3^L, and $(\gamma_3^L - \gamma_2^L)$ calculated from these by means of Eqs. (1) are given in Table III. Also listed is the light-hole mass value of $(0.047 \pm 0.005)m$ obtained by Cronburg *et al.*[35] from cyclotron-resonance experiments with submillimeter lasers. For comparison, the light-hole mass value of $(0.044 \pm 0.007)m$ and the heavy-hole mass value of $(0.33 \pm 0.013)m$ obtained by Walton and Mishra[36] from free-carrier reflectivity and Faraday rotation experiments at $T = 300$ K are also given in Table III.

While Stradling's cyclotron-resonance heavy-hole masses are in agreement with the values determined in the present experiment, his error estimates are considerably smaller. This points out the relative insensitivity of the present experiments, and of interband experiments in general, to the heavy-hole mass value. The values for m_{hh} for the present experiment were calculated from Eq. (3). This involves taking the difference between two terms of comparable magnitude, so that the small errors in the γ^L's produce larger errors in the value of m_{hh}.

The value of 1.3 ± 0.2 for the anisotropy parameter $(\gamma_3^L - \gamma_2^L)$ can be compared with the Shubnikov-de Haas measurements of Seiler and Becker.[37] They obtained a value of 11 ± 2 for the warping parameter $(L\text{-}M\text{-}N)$ in units of $(\hbar^2/2m)$. This parameter is simply related to the parameters B and C and to $(\gamma_3^L - \gamma_2^L)$ as follows:

$$L\text{-}M\text{-}N = 3\left[B - (B^2 + \tfrac{1}{3}C^2)^{1/2}\right] = 6(\gamma_3^L - \gamma_2^L). \qquad (23)$$

Equation (23) yields $(\gamma_3^L - \gamma_2^L) = 1.8 \pm 0.4$ for their measurements, which is in good agreement with the present result.

The present value of -7.8 ± 0.8 for g_c is slightly less than the recent value of -9.3 ± 0.3 obtained by

TABLE III. Comparison of the band-parameter values for GaSb determined in the present experiment with previously determined values. Effective-mass values are in units of the free-electron mass.

Band parameter	Present experiment	Magneto-absorption	Cyclotron resonance	Other experiments	Theory
m_c	0.042 ± 0.001	0.047 ± 0.003[a]	0.042 ± 0.002[b]	0.048 ± 0.002[c]	0.045[d]
		0.041[e]		0.049 ± 0.004[f]	0.040[g]
		0.045[h]			0.046[i]
					0.041[j]
m_{lh}	0.042 ± 0.002	0.041[h]	0.052 ± 0.004[k]	0.044 ± 0.007[l]	0.049[d]
			0.047 ± 0.005[m]		0.043[g]
					0.053[i]
					0.048[j]
$m_{hh}(100)$	0.29 ± 0.09		0.26 ± 0.04[k]		0.38[d]
$m_{hh}(110)$	0.36 ± 0.13		0.37 ± 0.04[k]		0.45[d]
$m_{hh}(111)$	0.40 ± 0.16		0.36 ± 0.03[k]	0.33 ± 0.013[l]	0.55[d]
γ_1^L	13.3 ± 0.4	14.5[h]	11.0[k]		11.2[d]
γ_3^L	5.7 ± 0.2	4.5[h]	4.4[k]		4.9[d]
$\gamma_3^L - \gamma_2^L$	1.3 ± 0.6		1.4[k]	1.8 ± 0.4[n]	1.0[d]
κ^L	3.5 ± 0.6	2.7[h]			3.1[d]
g_c	-7.8 ± 0.8	-6.5[h]		-9.3 ± 0.3[o]	-6.7[d]
m_{so}	0.12 ± 0.01				0.16[d]
g_{so}	-6.2 ± 3.2				-6.9[d]

[a]Reference 3. [e]Reference 31. [i]Reference 41. [m]Reference 35.
[b]Reference 32. [f]Reference 34. [j]Reference 42. [n]Reference 37.
[c]Reference 33. [g]Reference 39. [k]Reference 24. [o]Reference 38.
[d]Reference 40. [h]Reference 29. [l]Reference 36.

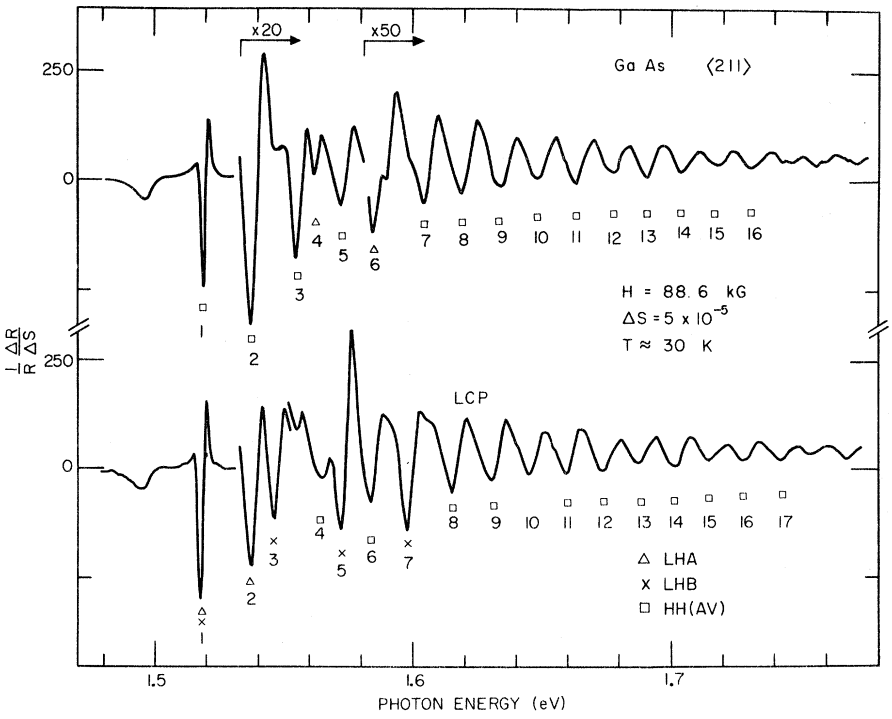

FIG. 17. Stress-modulated reflectivity spectra for GaAs in the Faraday configuration with the magnetic field along the ⟨211⟩ direction.

Hermann and Lampel[38] on the basis of conduction-electron spin resonance in p-type GaSb.

The last two rows of Table III contain our values for the splitoff band parameters m_{so} and g_{so}. These were calculated from Eqs. (11). This value for m_{so} and the value of Eq. (21) for m_c give $(0.031 \pm 0.001) \times m$ for the reduced effective mass for the conduction and splitoff valence bands. This is slightly less than the experimental value of $(0.0335 \pm 0.0003)m$ determined from our stress-modulated magnetoreflectivity data for the splitoff-band to conduction-band transition.[26] Those data also gave -12 ± 7 for the sum $(g_c + g_{so})$, while the above values for g_c and g_{so} yield the more precise value of -14 ± 3 for this sum. Finally, the theoretical values for the various parameters based on band-structure calculations for[39–42] GaSb are listed in the last column of Table III.

V. GALLIUM ARSENIDE

The result for the stress-modulated magnetoreflectivity for the fundamental edge of GaAs are shown in Fig. 17. The data were taken for the Faraday configuration with the magnetic field along the ⟨211⟩ direction. The spectra have about the same intensity as those for GaSb in Figs. 3 and 4. As can be seen in Fig. 17, transitions as high as 0.2 eV above the band gap were observed. By way of comparison, Vrehen's magnetoabsorption studies[4] on thin ($\sim 4\ \mu$) samples were limited to a spectral region of about 0.1 eV above the band gap. The line shapes of the GaAs spectra of Fig. 17 are both broader and more closely spaced than those of the GaSb spectra. The smaller separation is due to the larger value for the conduction-band effective mass $\sim 0.067m$,[4] as compared to the value of $0.042m$ for GaSb. This larger

TABLE IV. Experimentally observed transitions for GaAs in the Faraday configuration.

Label	Identification RCP	LCP
1	$a^-(1)a^c(0)$, $b^-(1)b^c(0)$	$a^+(-1)a^c(0)$, $b^+(-1)b^c(0)$
2	$a^-(2)a^c(1)$, $b^-(2)b^c(1)$	$a^+(0)a^c(1)$
3	$a^-(3)a^c(2)$, $b^-(3)b^c(2)$	$b^+(0)b^c(1)$
4	$a^+(1)a^c(0)$	$a^-(2)a^c(3)$, $b^-(2)b^c(3)$
5	$a^-(4)a^c(3)$, $b^-(4)b^c(3)$	$b^+(1)b^c(4)$
6	$a^+(2)a^c(1)$	$a^-(3)a^c(4)$, $b^-(3)b^c(4)$
7	$a^-(6)a^c(5)$, $b^-(6)b^c(5)$	$b^+(2)b^c(3)$
8	$a^-(7)a^c(6)$, $b^-(7)b^c(6)$	$a^-(5)a^c(6)$, $b^-(5)b^c(6)$
9	$a^-(8)a^c(7)$, $b^-(8)b^c(7)$	$a^-(6)a^c(7)$, $b^-(6)b^c(7)$
10	$a^-(9)a^c(8)$, $b^-(9)b^c(8)$	$a^-(7)a^c(8)$, $b^-(7)b^c(8)$
11	$a^-(10)a^c(9)$, $b^-(10)b^c(9)$	$a^-(8)a^c(9)$, $b^-(8)b^c(9)$
12	$a^-(11)a^c(10)$, $b^-(11)b^c(10)$	$a^-(9)a^c(10)$, $b^-(9)b^c(10)$
13	$a^-(12)a^c(11)$, $b^-(12)b^c(11)$	$a^-(10)a^c(11)$, $b^-(10)b^c(11)$
14	$a^-(13)a^c(12)$, $b^-(13)b^c(12)$	$a^-(11)a^c(12)$, $b^-(11)b^c(12)$
15	$a^-(14)a^c(13)$, $b^-(14)b^c(13)$	$a^-(12)a^c(13)$, $b^-(12)b^c(13)$
16	$a^-(15)a^c(14)$, $b^-(15)b^c(14)$	$a^-(13)a^c(14)$, $b^-(13)b^c(14)$
17	$a^-(16)a^c(15)$, $b^-(16)b^c(15)$	

effective mass may also contribute to the broader line shapes.

Because of the broadness of the structure and because of the relatively large exciton effects in GaAs, the data of Fig. 17 were not analyzed quantitatively. The recent photoluminescence studies on epitaxial GaAs by Gilleo *et al.*[43] established the exciton binding energy as (4.7 ± 0.4) meV which is more than twice the GaSb value of 2.2 meV estimated from Eq. (44) of Ref. 25. Hobden's magnetoabsorption study[44] of the lowest two transitions showed clearly their excitonic nature, and both Vrehen[4] and Narita[5] found it necessary to correct all of the transition energies they observed in magnetoabsorption for exciton effects. In the absence of a theory for the effect of excitons on transitions involving Landau levels of quantum number greater than 1 or 2, they had to use approximate corrections inferred from the calculations of Refs. 27 and 28.

In view of the above, only a qualitative interpretation of the GaAs spectra was made. By comparison with the GaSb spectra of Figs. 3 and 4, the minima in the GaAs spectra were associated with various allowed interband transitions. The identification of the minima is indicated in Fig. 17 by means of a symbol and a number directly below each prominent minimum. The symbol denotes the nature of the valence-band level involved and the number refers to the complete identification of the transition given in Table IV.

VI. CONCLUSION

This work represents the most detailed magneto-optical investigation to date of the direct transition in GaSb. The large number of Landau-level transitions observed with the stress-modulation technique has enabled us to quantitatively compare the data to the coupled-band theory of Pidgeon and Brown and to thus obtain an accurate self-consistent set of band parameters.

ACKNOWLEDGMENTS

We acknowledge the technical assistance of L. Sousa with the experiments and the computer programming performed by K. M. Reine. We thank Dr. U. Smith for helpful discussions during the course of this work and Dr. C. M. Wolfe for furnishing the GaAs sample used in these experiments. One of us (M. R.) acknowledges the financial assistance of a Fairchild Foundation Fellowship during part of this work.

---

†This paper is based on a Doctoral thesis submitted by M. Reine to the Physics Department, Massachusetts Institute of Technology. Work supported by the U. S. Air Force Office of Scientific Research.

*Present address: Honeywell Radiation Center, Lexington, Mass. 02173.

‡Also, Physics Department, Massachusetts Institute of Technology, Cambridge, Massachusetts, 02139.

§Now supported by the National Science Foundation.

[1]W. E. Engeler, H. Fritzche, M. Garfinkel, and J. J. Tiemann, Phys. Rev. Letters 14, 1069 (1965).

[2]R. L. Aggarwal, Phys. Rev. B 2, 446 (1970).

[3]S. Zwerdling, B. Lax, K. J. Button, and L. M. Roth, J. Phys. Chem. Solids 9, 320 (1959).

[4]Q. H. F. Vrehen, J. Phys. Chem. Solids 29, 129 (1968).

[5]S. Narita, M. Kobayashi, and N. Koikde, in *Proceedings of the IX International Conference on the Physics of Semiconductors, Moscow*, 1968 (Nauka, Leningrad, 1968), Vol. 1, p. 347.

[6]C. R. Pidgeon and R. N. Brown, Phys. Rev. 146, 575 (1966).

[7]L. M. Roth, B. Lax, and S. Zwerdling, Phys. Rev. 114, 90 (1959).

[8]R. L. Aggarwal, in *Semiconductors and Semimetals*, edited by R. K. Willardson and A. C. Beer (Academic, New York, to be published), Vol. 9.

[9]F. J. Ried, R. D. Baxter, and S. E. Miller, J. Electrochem. Soc. 113, 713 (1966).

[10]J. M. Luttinger, Phys. Rev. 102, 1030 (1956).

[11]E. Burstein, G. S. Picus, R. F. Wallis, and F. Blatt, Phys. Rev. 113, 15 (1959).

[12]G. Dresselhaus, A. F. Kip, and C. Kittel, Phys. Rev. 98, 368 (1955).

[13]E. O. Kane, J. Phys. Chem. Solids 1, 249 (1957).

[14]The deviation of Eqs. (10) and (11) from the Pidgeon and Brown formalism is given in Ref. 8.

[15]E. J. Johnson, I. Filinski, and H. Y. Fan, in *Proceedings of the International Conference on the Physics of Semiconductors, Exeter*, 1962 (The Institute of Physics and The Physical Society, London, 1962), p. 375.

[16]E. J. Johnson and H. Y. Fan, Phys. Rev. 139, A1991 (1965).

[17]C. B. Guillaume and P. Lavallard, Phys. Rev. B (to be published).

[18]F. H. Pollak and R. L. Aggarwal, Phys. Rev. B 4, 432 (1971).

[19]M. A. Habegger and H. Y. Fan, Phys. Rev. 138, A598 (1965).

[20]W. M. Becker, A. K. Ramdas, and H. Y. Fan, J. Appl. Phys. Suppl. 32, 2094 (1961).

[21]A. Gavini and M. Cardona, Phys. Rev. B 1, 672 (1970).

[22]Strictly speaking, these transitions involve the creation of excitons. In this paper, however, we treat them as occurring simply between Landau levels.

[23]J. G. Mavroides, in *Physics of Solids in Intense Magnetic Fields*, edited by E. D. Haidemenakis (Plenum, New York, 1969), pp. 206–232.

[24]R. A. Stradling, Phys. Letters 20, 217 (1966).

[25]M. Reine, Ph.D. thesis (Massachusetts Institute of Technology, 1970) (unpublished).

[26]M. Reine, R. L. Aggarwal, and B. Lax, Solid State Commun. 8, 35 (1970).

[27]Y. Yafet, R. W. Keyes, and E. N. Adams, J. Phys. Chem. Solids 1, 137 (1956).

[28]R. J. Elliot and R. Loudon, J. Phys. Chem. Solids 15, 196 (1960).

[29]E. Adachi, J. Phys. Chem. Solids 30, 776 (1968).
[30]J. Halpern, Bull. Am. Phys. Soc. 10, 594 (1965).
[31]B. Lax and J. G. Mavroides, in *Semiconductors and Semimetals*, edited by R. K. Willardson and A. C. Beer (Academic, New York, 1967), Vol. 3, pp. 321–401.
[32]D. A. Hill and C. F. Schwerdtfeger, Bull. Am. Phys. Soc. 15, 763 (1970).
[33]G. Bordure and R. Guastavino, Compt. Rend. 267, 860 (1968).
[34]H. Piller, in *Proceedings of the 7th International Conference on the Physics of Semiconductors* (Academic, New York, 1964), p. 297.
[35]T. L. Cronburg, K. J. Button, and B. Lax, Bull. Am. Phys. Soc. 15, 364 (1970).
[36]A. K. Walton and U. K. Mishra, J. Phys. C 1, 533 (1968).
[37]D. G. Seiler and W. M. Becker, Phys. Rev. 183, 784 (1969).
[38]C. Hermann and G. Lampel (unpublished).
[39]G. Bordure, Phys. Status Solidi 31, 673 (1969).
[40]C. W. Higginbotham, F. H. Pollak, and M. Cardona, in *Proceedings of the IX International Conference on the Physics of Semiconductors, Moscow*, 1968 (Nauka, Leningrad, 1968), Vol. 1, p. 57.
[41]H. I. Zhang and J. Callaway, Solid State Commun. 6, 515 (1968).
[42]M. L. Cohen and T. K. Bergstresser, Phys. Rev. 141, 789 (1966). Their effective masses are those shown in Table II of Ref. 41.
[43]M. A. Gilleo, P. T. Bailey, and D. E. Hill, Phys. Rev. 174, 898 (1968).
[44]M. V. Hobden, Phys. Letters 16, 107 (1965).

PHYSICAL REVIEW B VOLUME 5, NUMBER 8 15 APRIL 1972

Electron-Phonon Interactions in InSb Junctions

B. C. Cavenett
Department of Physics, University of Hull, England
(Received 20 September 1971)

Both oxide-coated and vacuum-cleaved InSb tunnel junctions have been prepared from single-crystal material with 7×10^{13} carriers/cm^3. Capacitance measurements at 4.2°K show that the barrier height is approximately the same as the energy gap at that temperature. The differential conductance of the junctions as a function of bias voltage shows at least 30 oscillations with a periodicity equal to the LO phonon energy. These oscillations show a striking resemblance to the oscillatory photoconductivity spectra observed in single-crystal InSb and, in fact, a satisfactory model proposed for the tunnel junctions involves a bulk conductance which changes in an oscillatory fashion due to the same mechanism as in the photoconductivity effect. Structure due to both the LA and TA phonons are observed near zero bias owing to inelastic tunneling processes. Further structure, which is particularly prominent in the vacuum-cleaved junctions, is interpreted as the transfer of carriers into the upper L_1 band and this gives an energy of 0.39 ± 0.01 eV between the conduction-band minima of L_1 and Γ_1 at the center of the zone.

I. INTRODUCTION

The first InSb tunnel diodes were made by Batdorf *et al.*[1] and a negative-resistance region (the Esaki characteristic) was observed between 78 and 273 °K. Chynoweth, Logan, and Wolff[2,3] have studied the magnetic field and temperature dependence of the tunneling in similarly prepared InSb p-n junctions. The observation of LO phonon interaction was first reported by Hall *et al.*[4–6] for III-V compound p-n tunnel junctions studied at 4.2 °K. A measurement of the derivative of the current, dI/dV, vs the voltage V for InSb showed structure when a phonon-assisted tunneling threshold of 24 meV was reached. Hall *et al.*[4] also reported the observation of a conductance minimum at zero bias and interpreted this as polaron formation. They ruled out the possibility that the conductance minimum was associated with acoustic phonon emission by temperature measurements of the tunnel current. However, this possibility has been reconsidered in a calculation by Bennett *et al.*[7] who have shown that such structure can result from TA phonon interactions which allow inelastic tunneling.

A theory of polar-phonon-assisted tunneling has been proposed by Dumke *et al.*,[8] who have considered the case of a direct phonon-assisted component of the current. It is emphasized that this is quite a different problem from the phonon-assisted indirect transitions which must be considered for indirect-gap materials such as Si and Ge.[9] However, the calculated ratio of phonon-assisted current to direct current was found to be 30 times smaller than the same ratio found from experiment.[4] An even greater discrepancy was observed when the magnitudes of the theoretical and experimental phonon-assisted tunneling currents were compared. The authors concluded that disagreement of the theory with experiment was not understood, although the effects of impurities within the